Chinese Journal of Chemical Engineering 67 (2024) 182–194

Contents lists available at ScienceDirect

Chinese Journal of Chemical Engineering

journal homepage: www.elsevier.com/locate/CJChE

Full Length Article

Uncertainty and disturbance estimator-based model predictive control for wet flue gas desulphurization system

Shan Liu [1], Wenqi Zhong [1,*], Li Sun [1], Xi Chen [1], Rafal Madonski [2]

[1] *School of Energy and Environment, Key Laboratory of Energy Thermal Conversion and Control of Ministry of Education, Southeast University, Nanjing 210096, China*

[2] *Faculty of Automatic Control, Electronics and Computer Science, Silesian University of Technology, Gliwise 44-100, Poland*

A R T I C L E I N F O

Article history:
Received 12 April 2023
Received in revised form
1 November 2023
Accepted 13 November 2023
Available online 15 December 2023

Keywords:
Desulphurization system
Disturbance rejection
Model predictive control
Uncertainty and disturbance estimator
Nonlinear system

A B S T R A C T

Wet flue gas desulphurization technology is widely used in the industrial process for its capability of efficient pollution removal. The desulphurization control system, however, is subjected to complex reaction mechanisms and severe disturbances, which make for it difficult to achieve certain practically relevant control goals including emission and economic performances as well as system robustness. To address these challenges, a new robust control scheme based on uncertainty and disturbance estimator (UDE) and model predictive control (MPC) is proposed in this paper. The UDE is used to estimate and dynamically compensate acting disturbances, whereas MPC is deployed for optimal feedback regulation of the resultant dynamics. By viewing the system nonlinearities and unknown dynamics as disturbances, the proposed control framework allows to locally treat the considered nonlinear plant as a linear one. The obtained simulation results confirm that the utilization of UDE makes the tracking error negligibly small, even in the presence of unmodeled dynamics. In the conducted comparison study, the introduced control scheme outperforms both the standard MPC and PID (proportional-integral-derivative) control strategies in terms of transient performance and robustness. Furthermore, the results reveal that a low-pass-filter time constant has a significant effect on the robustness and the convergence range of the tracking error.

1. Introduction

The worldwide development of science and technology is close to the utilization of energy. Fossil fuels are still the main energy today [1]. The utilization of fossil fuels is increasing in proportion to the rising global demand for energy. Sulfur oxides and other pollutants are released into the air as a result of the massive consumption of fossil fuels in coal-fired power plants, cement plants, steel plants, smelters, and other industrial processes, causing a negative impact on the environment and human health [2–5]. This impact intensifies with the increasing energy demand.

For the significant environmental impact caused by sulfur oxides, many countries have issued strict pollutant-emission regulations [6]. As a result, great challenges have been brought about to the desulphurization process. Studies have shown that many absorbents are effective, such as manganese hydroxide, magnesium hydroxide, and iodine [7–9]. However, the high cost of these absorbents prevents them from being widely used. Up to the present, wet flue gas desulphurization technology based on limestone or lime is still the predominant technology for its reliability [10]. Despite the fact that it is a mature technology, complicated desulphurization mechanisms and unknown factors in the operation process necessitate a rise in the consumption of absorbents to achieve a satisfying emission concentration, resulting in a decline of economic benefits. Therefore, a fast SO_2 emission concentration-tracking capability is required. Specifically, the slurry flow rate, among other parameters, needs to be adjusted using a controller based on the flue gas flow rate, flue gas composition, and other factors to ensure that the emission concentration meets the given regulation without being affected by other factors.

To address that challenge, many control techniques were proposed over the years to achieve efficient regulation of the

* Corresponding author. Tel.: +86 25 83794938; Fax: +86 25 83795508.
E-mail address: wqzhong@seu.edu.cn (W. Zhong).

https://doi.org/10.1016/j.cjche.2023.11.014
1004-9541/

desulphurization process, some of which are recalled in the following. For example, a decentralized control system, based on a linear multivariable model, was introduced in Ref. [11]. Here, however, the SO_2-tracking performance was influenced by the disturbance characteristics and parameters coupling. A radial basis function neural network-based PID (proportional-integral-derivative) controller was developed in Ref. [12] with online tuned parameters, which outperformed the traditional PID controller in the conducted tests. The disturbance rejection capability of a dynamic matrix control with feedforward was shown in Ref. [13] through an experiment performed on a pilot plant. A mixed logic dynamic model was developed in Ref. [14], based on which fast tracking of pH was realized by a predictive controller without taking into account the influence of the disturbance. To handle different disturbances, a multi-model predictive control strategy was tested in Ref. [15] on the desulphurization system, and satisfying control performance was obtained against multiple, simultaneously acting disturbances. A neural predictive controller was utilized in Ref. [16] as a feedback controller in a decentralized control strategy, where the robustness against inlet SO_2 concentration for SO_2 control relied on the feedforward term. By adding a feedforward term, the performance of the desulphurization system in the variation duration was improved in Ref. [17]. Considering the limitation of a single-plant mathematical model, a neural network was used in Ref. [18] to establish multiple local models, based on which a multi-model adaptive control method was used to control the desulphurization system.

From the conducted literature overview, effective control of the desulphurization system is still an open problem due to several challenges therein. The desulphurization process is essentially an acid-base neutralization reaction with strong nonlinearity [19]. Due to the overall complexity of the desulphurization process, it is difficult to establish an accurate nonlinear model. For the convenience of design and implementation, most of the currently available controllers are model-based and are derived based on linear plant models. The inevitable modeling uncertainties, coming from model linearization and other assumptions made about the plant mathematical model, further complicate the control process. When the operating conditions deviate far enough from the linearization point, the resulting modeling mismatch deteriorates the control performance. Moreover, fluctuations in the boiler load, sulfur content variations, measurement sensor failures, as well as parametric coupling and modeling mismatch, all cause significant perturbation to the system. Most of these disturbances are usually unknown and/or are unmeasurable, which further brings challenges to its control. It thus seems necessary to adopt a reliable control scheme for desulphurization systems in order to deal with their underlying uncertainties.

Many strategies have been presented to improve system robustness, such as active disturbance rejection control (ADRC) and linear regulator [20,21]. Though these control schemes have already been implemented in industrial processes, most of them require knowledge of the disturbance. So far, the model predictive control (MPC) algorithms have been successfully applied to many different industrial processes due to their capabilities of dealing with coupled, multivariable, and constrained systems [22,23]. However, the desulphurization system is, as already established, a disturbed and nonlinear process, and conventional linear-model predictive controllers show limitations when working in the presence of disturbances and modeling mismatch [24]. In general, the standard MPC techniques suppress disturbances through feedback regulation and not through dedicated controller design. Such architecture allows the control system to gradually suppress disturbances through relatively slow feedback adjustments but may cause system instability in the presence of strong disturbances [24]. It means that if no prior knowledge about the disturbance bound is available, the presence of strong and unmeasured disturbances will negatively affect the MPC capability to guarantee the desired performance. Hence, the use of the popular and industry-proven technique such as MPC should be “robustified” if the control of desulphurization system is considered. In other words, the MPC needs a dynamic compensator that would estimate and cancel all the uncertainties timely and accurately.

Adding a compensator to the controller by estimating and reducing the influence of uncertainties operating on the system is a promising scheme. Various researchers have proposed methods for disturbance attenuation, such as equivalent-input-disturbance, disturbance observer, and extended-state observer [25–27]. Disturbances need to meet specific assumptions in the equivalent-input-disturbance method. For the stabilization problem of nonlinear systems with bounded and unbounded disturbances, the author proposed disturbance estimator-based controllers, where filters are designed correspondingly. This method can estimate disturbances asymptotically and eliminate them exactly [28]. The uncertainty and disturbance estimator (UDE) technique does not depend on a precise system model and prior knowledge of disturbances affecting the controlled system [29]. All the uncertainties and disturbances are treated in the UDE scheme as a sole lumped term, which is simultaneously estimated and compensated. It can thus help to achieve satisfactory disturbance rejection even when the system is subjected to various interferences [30]. In recent years, UDE-based control schemes have been successfully utilized in many fields. It is well-known that a model-based controller cannot achieve satisfactory performance with uncertainties. Therefore, a UDE is used in the observer in a trajectory-tracking UDE-based feedback linearization controller for robot manipulators, which has been proven to be robust [31]. A UDE-based nonlinear controller has been successfully applied to the regulation of boost converter and the simulation result shows its superiority over a sliding mode controller [32]. In Ref. [33], a UDE-based controller was developed, and it was validated that it satisfies the requirements for quadrotors attitude control. A UDE-based multivariable controller was successfully designed and implemented in the tracking control of aeroengine, based on the nonlinear affine model [34]. In addition, the UDE technique has also been extended to address time-delay problems. A truncated predictive controller based on an UDE was proposed in response to input delay and bounded disturbance problems of the complex dynamical networks [35]. Besides its disturbance estimation and rejection capabilities, the UDE is a practically appealing algorithm due to its implementation simplicity as well as independence from an accurate knowledge of the derivatives of the state vector or the disturbance.

Therefore, motivated by the need for an effective robust control strategy for the challenging desulphurization system, in this work, a combination of the UDE and the MPC is proposed. The contribution of the paper is the development of a control solution that addresses the problems of conventional MPC of handling disturbances and modeling mismatch in the desulphurization system. The proposed UDE–MPC control structure is realized by first formulating the desulphurization system control problem under the framework of MPC. Then, to overcome the shortcomings of standard MPC, the system disturbances and modeling mismatch are treated collectively as a single perturbation term to be estimated and compensated as the system uncertainties. Finally, the performance of the standard MPC is improved by adding the UDE that handles the assumed uncertainty in real time. The introduction of the UDE as a compensator in the linear MPC potentially creates a synergic effect, improving the performance of conventional MPC controller and combining the desired characteristics of both methods, including the following:

(1) Robust control performance due to on-line disturbance estimation and cancellation;
(2) No requirements for the prior knowledge of uncertainties and disturbance as well as the derivative of the system state;
(3) Capability of handling multiple-input and multiple-output systems;
(4) Straightforward implementation and tuning.

These advantages potentially make the proposed combination convenient for industrial use and can satisfy the desulphurization system's stringent control requirements. In order to verify the efficacy of the proposed UDE-MPC control approach, a multi-criteria simulation study is conducted in this work. The performance of the proposed methodology is compared with results of a conventional MPC. Additionally, the results are compared with those of a standard PID controller, which is the most common feedback strategy in the industry and is a first-choice solution of practitioners.

The rest of the paper is organized as follows. Section 2 recalls some necessary information about the desulphurization system, introduces the control objectives (with difficulties in realizing them), as well as presents the system mathematical model. Section 3 shows the derivation of the proposed UDE–MPC control approach. Section 4 presents the simulation results of using the proposed UDE–MPC control structure on the desulphurization system and compares its performance with selected mainstream techniques. This section also contains an analysis of an interesting effect the time constant has on disturbance suppression. Section 5 concludes the work.

2. Preliminaries

2.1. Working principle of a desulphurization system

In the desulphurization process, the limestone slurry is sprayed into the absorption zone through nozzles of spray layers and gas distribution trays and contacts with the upward raw flue gas. This way of gas–liquid flow enhances the chemical reaction and improves the SO_2 removal efficiency. To keep the pH level of the slurry at a suitable value (*i.e.*, to guarantee certain desired removal performance), the fresh slurry, ground by ball mill, is continuously sent to the oxidation tank. In the oxidation zone, the oxygen in the blown air enhances the oxidation process of the falling slurry droplets. Finally, the reactants are discharged from the oxidation zone and are dehydrated to obtain by-products. The principle of the desulphurization process is illustratively shown in Fig. 1, and more detailed information on it can be found in Refs. [36,37].

2.2. Control objectives

In the desulphurization system, the SO_2 emission concentration and the pH value of the slurry are important parameters to measure the efficiency and the equipment security of the system. A high pH value is beneficial for the absorption of SO_2 but inhibits the dissolution of the limestone and promotes scaling in the tower. A small pH value increases the solubility of the limestone and inhibits the absorption of SO_2. According to Ref. [37], an optimal range of the pH is 5–6. In principle, meeting stricter SO_2 emission limits means higher operating costs. The main purpose of introducing advanced control schemes is to reduce the influence of SO_2 emission concentration more effectively than done through conventional control strategies, thus allowing a smaller SO_2 emission margin and reducing operating costs.

This means that an effective desulphurization-process control system should be designed to facilitate the realization of the three following control objectives. First, to satisfy environmental protection requirements, the SO_2 emission concentration should strictly comply with the emission regulations. Then, for the acid-base neutralization process, to protect the equipment and maintain the desulphurization effect, the pH value of the slurry should be adjusted to a suitable range. Finally, in addition to the nonlinearity and the coupling of the system, the desulphurization system is also affected by various disturbances, which bring about great challenges to the system stability. Therefore, the SO_2 emission concentration and the pH value of the slurry should be made impervious to the effects of external disturbances.

2.3. System mathematical modeling

The limestone dissolution, gas absorption, oxidation, and gypsum crystallization are the main chemical reactions in the desulphurization process. The absorption and oxidation zones are regarded as the plug flow reactor and continuously stirred tank reactor, respectively. For the modeling purpose, the micro reaction in the desulphurization process is ignored. According to the ion balance and mass balance, the dynamic equations can be established in each zone. Balancing between modeling accuracy and simplicity, the following models can be established for key elements of the system.

SO_2 absorption is controlled by gas phase, liquid phase, and the chemical reaction; the absorption rate can be described as expressed in Eq. (1). CO_2 is an insoluble gas, and the absorption rate is mainly controlled by liquid phase [38]:

$$r_{SO_2} = \alpha\left(p_{SO_2} - H_{SO_2}C_{SO_2}\right)\left[1/k_{G,SO_2} + H_{SO_2}/\left(\beta_{SO_2}k_{L,SO_2}\right)\right]^{-1} \tag{1}$$

$$r_{CO_2} = k_{L,CO_2}\beta_{CO_2}\alpha\left(p_{CO_2}/H_{CO_2} - C_{CO_2}\right) \tag{2}$$

The limestone dissolution rate is considered as the function of the relative supersaturation [36]:

$$r_{d,CaCO_3} = \left(C_{Ca^{2+}}\cdot C_{CO_3^{2-}} \Big/ K_{SP,CaCO_3} - 1\right)k_{d,CaCO_3} \tag{3}$$

The crystallization rate is obtained by the empirical expression [39,40]:

$$r_{c,CaSO_4} = 1.1\times10^{-4}A\left(C_{Ca^{2+}}\cdot C_{SO_4^{2-}} \Big/ L_{CaSO_4} - 1\right) \tag{4}$$

The oxidation rate of sulfite ions is affected by pH and the concentration of Mn^{2+} and other ions. Considering that ions precipitate quickly with gypsum, the oxidation rate is expressed as Eq. (5).

$$r_{ox} = k_{ox}\left(C_{HSO_3^-} + C_{SO_3^{2-}}\right)^{1.5} \tag{5}$$

The absorption zone is considered to be in a quasi-steady state as the residence time of the gas phase and liquid phase is short. Based on the rate equations mentioned earlier and the mass balance, the variation of ion concentration in the slurry droplet after passing through the absorption zone can be expressed as follows:

$$\Delta C_i = \tau\sum r_i \tag{6}$$

The oxidation zone can be regarded as a well-mixed vessel, and the components in the oxidation tank are well distributed. The dynamic ion concentration in the oxidation zone can be described as expressed in Eq. (7) [40].

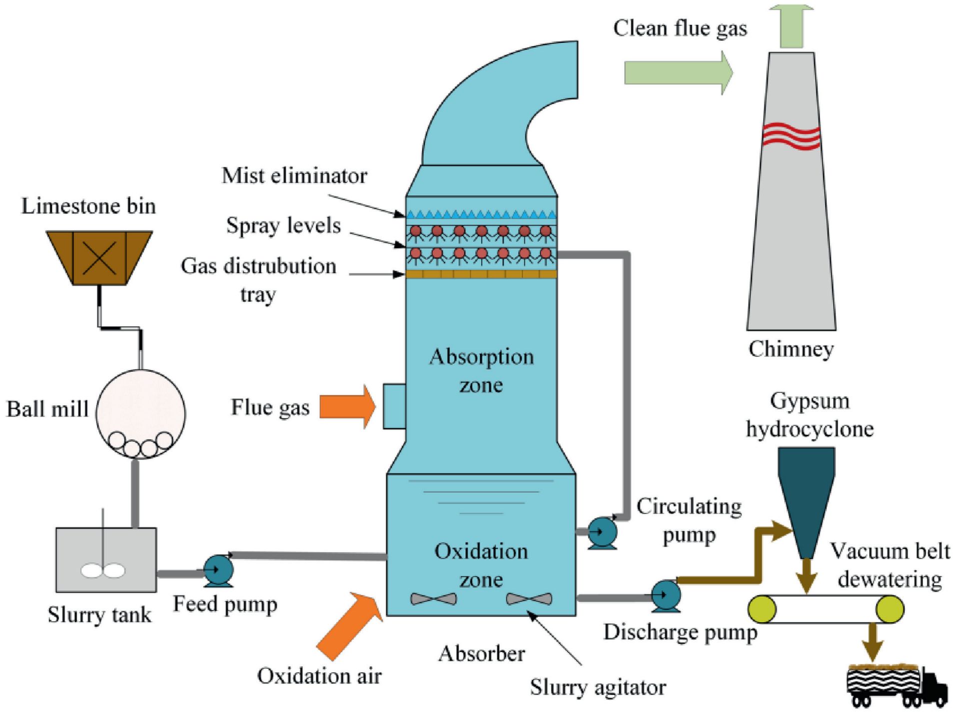

Fig. 1. The principle schematic of the desulphurization process.

$$\frac{\mathrm{d}C_i}{\mathrm{d}t}=\frac{Q_{\mathrm{in}}C_{\mathrm{in}}+Q_{\mathrm{fal}}C_{\mathrm{fal}}-Q_{\mathrm{r}}C_{\mathrm{r}}-Q_{\mathrm{out}}C_{\mathrm{out}}}{V_{\mathrm{t}}}+\sum r_i \tag{7}$$

where C_i represents the ions concentration in the slurry, Q_{in} is the flow rate of the fresh slurry bumped in the tank, Q_{fal} denotes the flow rate of the spraying slurry, Q_{r} is the flow rate of the recirculating slurry, and Q_{out} represents the flow rate of the waste slurry.

The clean flue gas after desulphurization is discharged into the chimney together with the forced oxidation air. Therefore, the SO_2 emission concentration can be described as follows:

$$m_{\mathrm{SO_2,out}}=\frac{G\cdot y_{\mathrm{SO_2}}+K_{\mathrm{G}}\cdot\alpha\cdot H_{\mathrm{SO_2}}\cdot C_{\mathrm{SO_2}}\cdot V_{\mathrm{ta}}}{G+G_{\mathrm{air}}+K_{\mathrm{G}}\cdot\alpha\cdot P\cdot V_{\mathrm{ta}}} \tag{8}$$

for

$$y_{\mathrm{SO_2}}=m_{\mathrm{SO_2,in}}-\tau(N_{\mathrm{SO_2}}\cdot Q_{\mathrm{r}}/G) \tag{9}$$

whereas the desulphurization efficiency can be expressed as follows:

$$\eta=\frac{G\cdot m_{\mathrm{SO_2}}-(G+G_{\mathrm{air}})\cdot m_{\mathrm{SO_2,out}}}{G\cdot m_{\mathrm{SO_2}}}. \tag{10}$$

The main influencing factors of the hydrogen-ion concentration in the slurry are the amount of SO_2 absorbed and the consumption of calcium carbonate, which can be described as follows:

$$\frac{\mathrm{d}C_{\mathrm{H^+}}}{\mathrm{d}t}=\frac{2\left(\frac{W_{\mathrm{SO_2}}}{M_{\mathrm{SO_2}}}-\frac{W_{\mathrm{CaCO_3}}}{M_{\mathrm{CaCO_3}}}\right)}{V_{\mathrm{t}}} \tag{11}$$

$$y_{\mathrm{pH}}=-\lg C_{\mathrm{H^+}} \tag{12}$$

where $W_{\mathrm{SO_2}}$ denotes the amount of SO_2 absorbed from the flue gas and $W_{\mathrm{CaCO_3}}$ represents the amount of calcium carbonate consumed in the desulphurization process, with

$$W_{\mathrm{SO_2}}=G\cdot\rho_{\mathrm{SO_2,in}}\cdot\eta \tag{13}$$

$$W_{\mathrm{CaCO_3}}=Q_{\mathrm{in}}\cdot\rho_{\mathrm{CaCO_3}} \tag{14}$$

Many parameters in the desulphurization process affect the pH and the SO_2 emission concentration, such as parameters of the flue gas at the inlet of the absorption tower, the flow rate, the density of the limestone slurry, and the operation condition of the equipment. The characteristic of the flue gas is constrained by the boiler load, flue pipe structure, and SO_2 concentration and is usually regarded as a disturbance in the controller design.

Considering the control objectives and various influencing factors, the SO_2 emission concentration ($m_{\mathrm{SO_2,out}}$) and the pH value of the slurry (y_{pH}) are selected as the controlled variables, and the slurry flux (Q_{in}) and the recirculating slurry flux (Q_{r}) are selected as the manipulated variables. Therefore, the mathematical model of the desulphurization system can be represented as a following nonlinear dynamics:

$$\begin{cases}\dot{\boldsymbol{x}}=f(\boldsymbol{x},\boldsymbol{u})\\ \boldsymbol{y}=g(\boldsymbol{x},\boldsymbol{u})\end{cases} \tag{15}$$

where $\boldsymbol{u}=[Q_{\mathrm{in}},Q_{\mathrm{r}}]^{\mathrm{T}}$ denotes the control input vector, $\boldsymbol{y}=\left[m_{\mathrm{SO_2,out}},y_{\mathrm{pH}}\right]^{\mathrm{T}}$ is the system output vector, and $\boldsymbol{x}=\left[C_{\mathrm{CO_2}},C_{\mathrm{HCO_3^-}},C_{\mathrm{CO_3^{2-}}},C_{\mathrm{SO_2}},C_{\mathrm{HSO_3^-}},C_{\mathrm{SO_3^{2-}}},C_{\mathrm{HSO_4^-}},C_{\mathrm{H^+}},C_{\mathrm{Ca^{2+}}},C_{\mathrm{CaSO_4}},C_{\mathrm{CaCO_3}}\right]^{\mathrm{T}}$ is the state variable, which is composed of the ion concentration of the slurry in the oxidation tank.

2.4. Control difficulties

It has been already mentioned that the considered desulphurization system is a disturbed, nonlinear system with coupled parameters. To analyze the significance of those characteristics on the control performance, a detailed analysis is conducted next.

2.4.1. Nonlinearity

The desulphurization process is a neutralization reaction, which has intrinsic nonlinear characteristics. Due to the limitation of emission concentration, equipment life, and the demand for gypsum production, the pH value of the slurry in the oxidation tank fluctuates in a small range, generally around 5.2–5.8, where the system has a certain nonlinearity. Fig. 2 shows the open-loop response of the system, where it can be seen that system responses vary under different boiler loads, even under the same slurry and flue gas quality, thus revealing the significant nonlinear nature of the process.

2.4.2. Parameters coupling

Fig. 3 shows an open-loop response of the desulphurization system with different input disturbances. One can notice that the pH value jumps in opposite trend at the time of the SO_2 emission concentration variation, demonstrating the effect of system coupling.

To analyze the interactions between variables, the notion of relative gain array (RGA) is introduced [41]. The elements of the RGA matrix are defined as follows:

$$\lambda_{ij} = \frac{(\partial y_i/\partial u_j)_u}{(\partial y_i/\partial u_j)_y} = \frac{\text{open}-\text{loop gain}}{\text{closed}-\text{loop gain}} \tag{16}$$

interpreted as the ratios of the system open-loop and closed-loop gains. To describe the interactions in the dynamic system, the frequency-dependent RGA can be defined as follows:

$$\mathrm{RGA}(\boldsymbol{G}) = \boldsymbol{G}(j\omega)\otimes\boldsymbol{G}^{-1}(j\omega)^{\mathrm{T}} \tag{17}$$

where $\otimes$ denotes the Schur product.

Fig. 4 shows the frequency-dependent gain curve of the desulphurization system with inputs $Q_{in}(u_1)$ and $Q_r(u_2)$ and outputs $m_{SO_2,out}(y_1)$ and $y_{pH}(y_2)$. One can see that the coupling degree between system variables varies with frequency and that the coupling can be ignored at high frequency. However, the RGA is negative at low frequency, indicating that there is positive feedback on the corresponding channel. This kind of coupling can easily bring instability to the closed-loop system. Furthermore, it can be concluded that a diagonal pairing should be chosen, *i.e.*, $Q_{in}(u_1)$ used to control $y_{pH}(y_2)$ and $Q_r(u_2)$ used to control $m_{SO_2,out}(y_1)$.

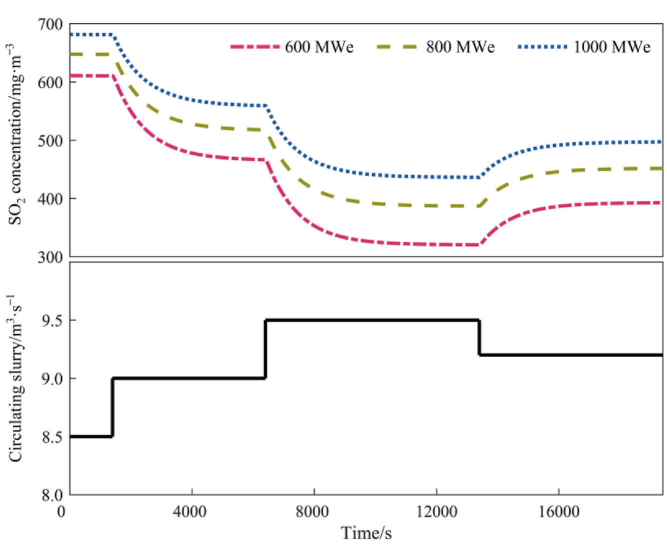

Fig. 2. Open-loop step response of the desulphurization system at different boiler load.

2.4.3. Disturbances

In real-world operation, the desulphurization system also suffers from impact of various unmeasurable disturbances. The boiler load fluctuation, flue gas concentration fluctuation, valve failure, sensor failure, fresh slurry quality, the composition of raw materials, and measurement error will all bring unwanted fluctuations to the slurry quality in the oxidation tank and have influence on the SO_2 removal effect. To suppress the influence of the unmeasurable disturbance, a safety margin between the actual SO_2 emission concentration and the SO_2 emission limit is artificially set. However, the resultant control scheme increases the desulphurization cost and runs in the direction opposite to the demand of the industrial processes.

3. Main Result: UDE-MPC Solution for Desulphurization System

In this section, the UDE-MPC structure is proposed to achieve satisfactory performance in the control of desulphurization system.

3.1. Model predictive control

In the MPC methodology, the input signal to the plant is obtained by solving an objective function, which usually consists of some predefined tracking objectives and system constraints. The control objectives of the desulphurization system are to track the set values of SO_2 emission concentration and the pH. Therefore, the form of tracking MPC is selected as shown in Eq. (18). For the considered nonlinear desulphurization system, $\begin{cases}\boldsymbol{x}_{k+1} = f(\boldsymbol{x}_k, \boldsymbol{u}_k)\\ \boldsymbol{y}_k = g(\boldsymbol{x}_k, \boldsymbol{u}_k)\end{cases}$ is the discrete from of Eq. (15) and the control signal $\boldsymbol{u}_k = [Q_{in}, Q_r]^{\mathrm{T}}$ is calculated by minimizing the following objective function:

$$\min_{u(i)} \sum_{i=k}^{k+N-1} \lambda_i \|\boldsymbol{r}(i) - \boldsymbol{y}(i)\|_q + \sum_{i=k}^{k+N-1} \beta_i \|\Delta\boldsymbol{u}(i-1)\|_q \tag{18}$$

with constraints

$$\boldsymbol{x}(i+1) = f(\boldsymbol{x}(i), \boldsymbol{u}(i)) \tag{19}$$

where

$$x(0) = x_0 \tag{20}$$

$$u_{\min} \le \boldsymbol{u}(i) \le u_{\max}, i = 0, 1, \cdots, N-1 \tag{21}$$

$$y_{\min} \le \boldsymbol{x}(i) \le y_{\max}, i = 0, 1, \cdots, N-1 \tag{22}$$

$$\boldsymbol{y}(N) \in Z, i = 0, 1, \cdots, N-1 \tag{23}$$

In the above formulation, $\boldsymbol{r}$ is the vector of the desired SO_2 emission concentration and the desired slurry pH value, and λ_i represents the output weighting coefficient, which is the reciprocal of the expected error of SO_2 emission concentration ($m_{SO_2,out}$) and pH value (y_{pH}). β_i denotes the suppression factor used to limit control actions.

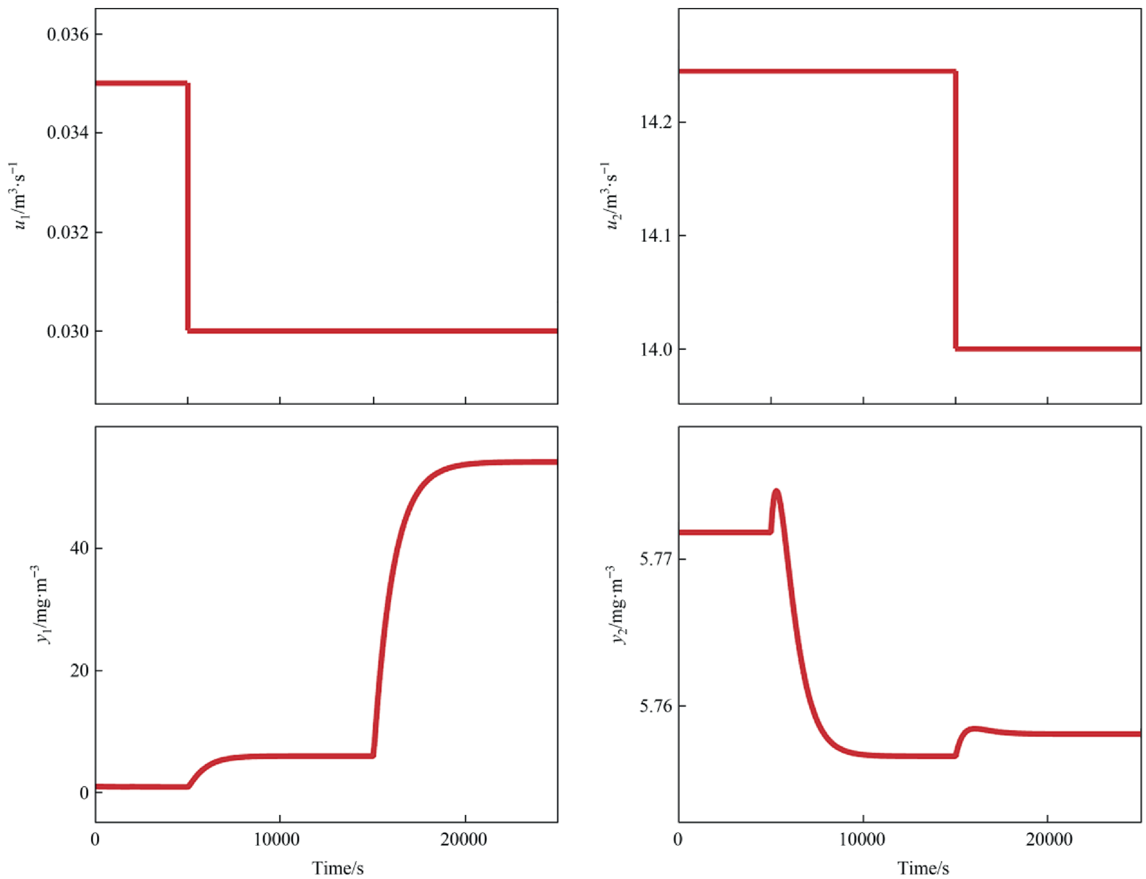

Fig. 3. Open-loop response of the desulphurization system with different input disturbances.

Remark 1. Generally, the stability of MPC can be guaranteed by infinite predictive time domain, terminal equality constraints, terminal constraint set, and taking the objective function as a Lyapunov function [42–45]. In this paper, the terminal constraint set is constructed, and the objective function is constructed as Lyapunov function to ensure the stability of the system.

In the proposed design, the parameter coupling is regarded as part of the acting disturbance, which can be removed during the dynamic optimization by expressing it as a model error. The feedback channel can correct the SO_2 emission concentration and the slurry pH value when there are deviations from the target values; however, this brings fluctuation to the desulphurization system. Another way to reject disturbances is by introducing the feedforward compensation, in which the disturbance is measured and then canceled out before the controlled variable changes. This approach is, however, only applicable to scenarios with prior knowledge about the disturbances. The unmeasurable disturbances and various modeling uncertainties (under different boiler loads) are inevitable in practice, and they limit the controller capability to meet a satisfactory performance of the governed desulphurization system. To address this drawback, the standard MPC is enhanced in this work with the UDE, which is described next.

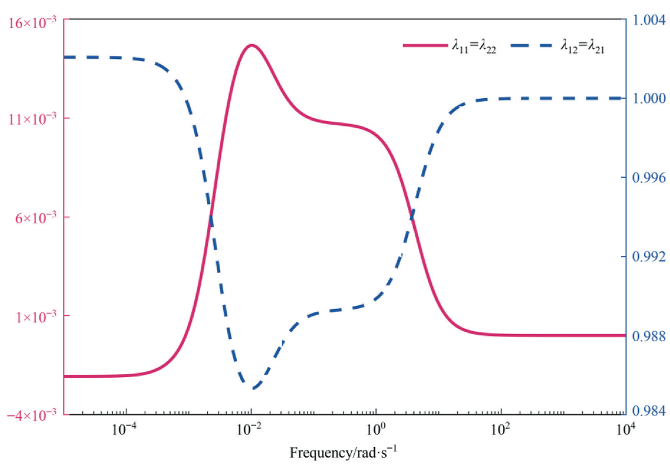

Fig. 4. Frequency-dependent RGA of the desulphurization system.

3.2. *Combination with uncertainty and disturbance estimator*

To reject the uncertainty and disturbance and to improve the robustness of the desulphurization system, the disturbance compensation term is introduced in the MPC framework. Compared to a conventional feedforward compensation, the UDE does not require prior knowledge of disturbances and uncertainties [29]. In this work, the nonlinear desulphurization system is regarded as a linear system disturbed, with lumped uncertainties, that comprises of system nonlinear characteristics, external disturbances, and unknown system dynamics. The UDE scheme is used to observe and compensate uncertainties in real time. Therefore, the control law u of the desulphurization system consists of two parts:

$$\boldsymbol{u}_{\text{total}} = \boldsymbol{u}_{\text{d}} + \boldsymbol{u} \tag{24}$$

where $\boldsymbol{u}$ is the solution of the conventional MPC (Eq. (18)), and $\boldsymbol{u}_{\text{d}}$ is the uncertainty and disturbance estimator derived from the system dynamic characteristics.

In order to obtain $\boldsymbol{u}_{\text{d}}$, the nonlinear desulphurization system model from Eq. (15) is first reformulated as a linear system with lumped uncertainties:

$$\begin{cases} \dot{\mathbf{x}} = \boldsymbol{Ax} + \boldsymbol{Bu} + \boldsymbol{h}(\boldsymbol{x},\boldsymbol{u},\boldsymbol{d}) \\ \boldsymbol{y} = g(\boldsymbol{x},\boldsymbol{u}) \end{cases} \tag{25}$$

where $\boldsymbol{A}$ is the known desulphurization system state matrix, $\boldsymbol{B}$ is the known control matrix, $\boldsymbol{h}(\boldsymbol{x},\boldsymbol{u},\boldsymbol{d})$ denotes the unknown terms, and d represents the unpredictable disturbance. The lumped uncertainties can be expressed as follows:

$$h(\boldsymbol{x},\boldsymbol{u},\boldsymbol{d}) = \dot{\mathbf{x}} - \boldsymbol{Ax} - \boldsymbol{Bu} \tag{26}$$

Therefore, the lumped uncertainties compensation on the input is

$$\boldsymbol{u}_h = -\boldsymbol{B}^{+}h(\boldsymbol{x},\boldsymbol{u},\boldsymbol{d}) = -\boldsymbol{B}^{+}(\dot{\mathbf{x}} - \mathbf{Ax} - \mathbf{Bu}) \tag{27}$$

and in the s-domain, it takes the following form:

$$\boldsymbol{U}_h = \boldsymbol{B}^{+}[(\boldsymbol{A} - s\boldsymbol{I})\boldsymbol{X}(s) + \boldsymbol{BU}(s)] \tag{28}$$

where $\boldsymbol{B}^{+} = \left(\boldsymbol{B}^{\text{T}}\boldsymbol{B}\right)^{-1}\boldsymbol{B}^{\text{T}}$ is the pseudoinverse of $\boldsymbol{B}$.

From Eq. (27), the unknown dynamics and disturbances could be obtained from the known system dynamics and input signal. However, the lumped uncertainties compensation (29) cannot be used in the control law directly. The lumped uncertainties compensation can be approximated using a proper filter G_{f}:

$$\boldsymbol{u}_{\text{d}} \approx \boldsymbol{B}^{+}[(\boldsymbol{A} - s\boldsymbol{I})\boldsymbol{X}(s) + \boldsymbol{BU}(s)]G_{\text{f}}(s) \tag{29}$$

The disturbances and the unknown dynamics during the desulphurization system operation are generally located in the low-frequency range. Hence, G_{f} is chosen as a low-pass filter that has a large-enough bandwidth to cover the spectrum of the desulphurization system dynamics and disturbances:

$$G_{\text{f}}(s) = \frac{1}{T_{\text{f}}s + 1} \tag{30}$$

where T_{f} is the filter time constant (design parameter). It is assumed that the frequency upper limit is w_{f} ($w_{\text{f}} = 1/T_{\text{f}}$), then

$$G_{\text{f}} = \frac{1}{\frac{1}{w_{\text{f}}}s + 1} = \begin{cases} 1, & w < w_{\text{f}} \\ 0, & w > w_{\text{f}} \end{cases} \tag{31}$$

Finally, the estimation error of the UDE can be straightforwardly calculated as follows:

$$\boldsymbol{e} = \boldsymbol{B}^{+}[(\boldsymbol{A} - s\boldsymbol{I})\boldsymbol{X}(s) + \boldsymbol{BU}(s)]\left(1 - G_{\text{f}}(s)\right) \approx \begin{cases} 0, & w < w_{\text{f}} \\ 0, & w > w_{\text{f}} \end{cases} \tag{32}$$

As seen from Eq. (24), the UDE control scheme does not require prior knowledge of the uncertainties. The estimated value $\boldsymbol{u}_{\text{d}}$ is used as the feedforward compensation to offset the adverse effects of the unknown dynamics and disturbances on the desulphurization system output. As seen from Eqs. (28) and (30), $\boldsymbol{u}_{\text{d}} \approx -\boldsymbol{B}^{+}h(\boldsymbol{x},\boldsymbol{u},\boldsymbol{d})G_{\text{f}}(s)$, and $\boldsymbol{u}_{\text{d}}$ will converge to the difference between the desulphurization system and the linearized model at the input of the system. Moreover, the UDE control scheme adopts the desulphurization system state x to observe the lumped uncertainties, but the ion concentration cannot be measured timely. Hence, a standard Kalman filter is chosen to observe the state of the desulphurization system. It is divided into two recursive processes including prediction and correction, the detailed introduction and equations of which are omitted here but shown in details in Refs. [46,47]. Finally, the proposed control scheme, combining MPC and UDE, is shown in Fig. 5.

Certainly, the practical application of this control design also faces challenges. This method does not depend on model accuracy or disturbance information precision but does require knowledge of the disturbance's bandwidth. In situations where operational complexity increases and unforeseen uncertainties and interferences are encountered, the implementation of the controller becomes more complex, necessitating adjustments to the designed filter. Additionally, the choice of reference models and feedback gains has a significant impact on the controller's implementation.

4. Simulation Validation and Analysis

In this section, the simulation results of a nonlinear desulphurization system in a coal-fired power plant using the UDE-MPC control scheme are presented. To check the efficacy of the proposed approach and its robustness, a comparison study is conducted between the proposed control scheme, standard MPC solution, and a conventional industrial PID controller. From Ref. [48], we know that the PID controller is still common in thermal power plants due to its simplicity, hence it is chosen for comparison. The predictive model in the standard MPC scheme is chosen as a linear model, which is obtained by linearizing the nonlinear system at a steady-state point. The PID control scheme is implemented using two independent loops, one using $Q_{\text{in}}(u_1)$ to control $y_{\text{pH}}(y_2)$ and the other using $Q_{\text{r}}(u_2)$ to control $m_{\text{SO}_2,\text{out}}(y_1)$. Considering an actual, industrial scenario, a low-frequency disturbance is assumed in the tests. In addition, the influence of the UDE-filter time constant on the control effect is investigated. Considering the system dynamic response shown in Fig. 3, the prediction horizon is selected as 100 s. In addition, the sampling time and control horizon of MPC are set to 20 s and 8 s, respectively. λ_i is set to diag[0.6 1] and β_i is selected as diag[0.1 0.4]. In the PID controller, the proportional, integral, and derivative coefficients are tuned based on a popular Ziegler–Nichols method. Since the disturbances in the desulphurization are generally located in the low-frequency range, T_{f} of the UDE is chosen as 0.0001 s so that the bandwidth is

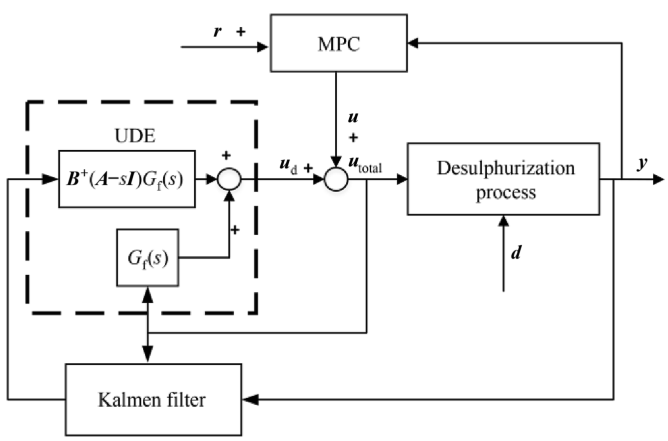

Fig. 5. Block diagram of the proposed UDE-MPC control architecture.

large enough to cover the spectrum of disturbances. The pH value of the slurry does not need to be kept constant, but within a reasonable range, allowing for more flexibility in SO_2 control.

4.1. Robustness tests

To illustrate the robustness of the proposed control scheme, two scenarios of set-points for the desulphurization system are simulated: SO_2 emission concentration limit is constant and SO_2 emission concentration limit varies. Considering the operational conditions, the external disturbances are considered as sinusoidal waves corrupted with bounded white noise.

4.1.1. Case I: SO_2 emission concentration limit remains constant

Although the pH and SO_2 emission concentration are the controlled variables, the latter is the main objective, as determined by the chosen weighting coefficient in Table 1. In the tests, limits on actuators (valve opening of slurry pump and circulating pumps) and emission regulation (SO_2 emission limit is 35 $mg\cdot m^{-3}$ in this paper) are taken into consideration. Therefore, simulations under two distinct input disturbance scenarios (large and small amplitude disturbances) are examined to validate the effectiveness of the proposed control scheme. The large amplitude disturbance refers to the disturbance with fluctuation amplitude of 0.01 $m^3\cdot s^{-1}$ and 0.5 $m^3\cdot s^{-1}$ added in Q_{slu} and Q_{cir}, respectively. Similarly, small amplitude disturbance refers to 0.001 $m^3\cdot s^{-1}$ and 0.1 $m^3\cdot s^{-1}$.

Fig. 6 shows the simulation results in the presence of small-amplitude disturbances under three tested control schemes (PID, MPC, and the proposed UDE-MPC). As seen in Fig. 6(a), the UDE-MPC control scheme outperforms the other controllers in terms of SO_2 emission concentration tracking. Two performance indices, namely average tracking error and maximum tracking error, are used to determine the disturbance rejection quality in Table 1. The comparison of system disturbance and compensation estimated by UDE are shown in Appendix. The proposed UDE-MPC scheme has smaller SO_2 concentration fluctuation amplitudes than PID and MPC. This demonstrates that UDE is capable of effectively estimating and compensating lumped uncertainties including system nonlinearity, parameter coupling, and external disturbances.

Next, large-amplitude disturbances are used in the simulation to further test the robustness of the compared control methods. Fig. 7 and Table 1 illustrate the results of the comparison. Similar to Fig. 6, the proposed method results in reduced tracking error. It outperforms the MPC and PID in terms of disturbance rejection, even when large-amplitude disturbances are present. The UDE–MPC controller has the least departure from the expected SO_2 emission limit in the two disturbance scenarios. This means that it is not necessary to maintain an excessive control margin. It also shows the robustness of the desulphurization process control system as well as its positive impact on the operational economy of the entire process.

Table 1
Tracking error of SO_2 between different control schemes

Performance index	Small amplitude disturbance			Large amplitude disturbance		
	PID	MPC	UDE-MPC	PID	MPC	UDE-MPC
ATE/$mg\cdot m^{-3}$	0.0064	0.0301	9.8558×10^{-6}	0.0276	0.1025	0.0029
MTE/$mg\cdot m^{-3}$	0.0233	0.1290	1.6884×10^{-5}	0.0847	0.4341	0.0597

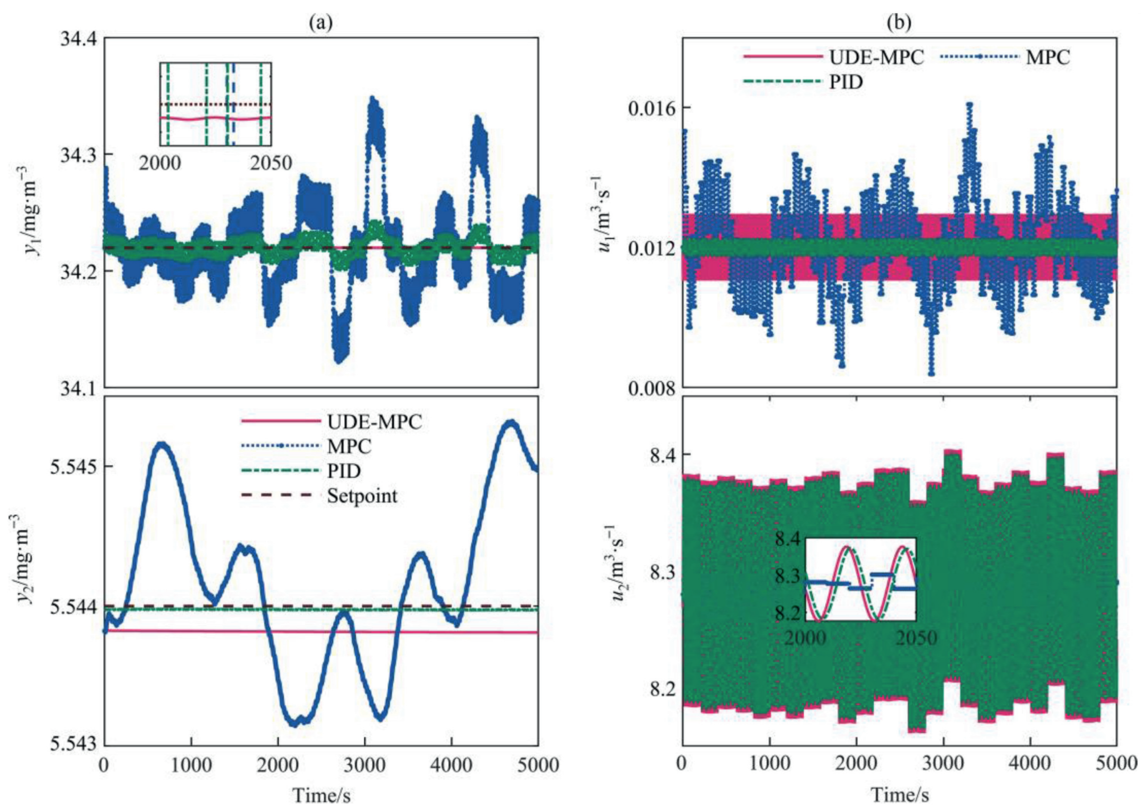

Fig. 6. The desulphurization system simulation results in the presence of small-amplitude external disturbances under different control schemes, with (a) response curves of controlled variables and (b) variations of manipulated variables.

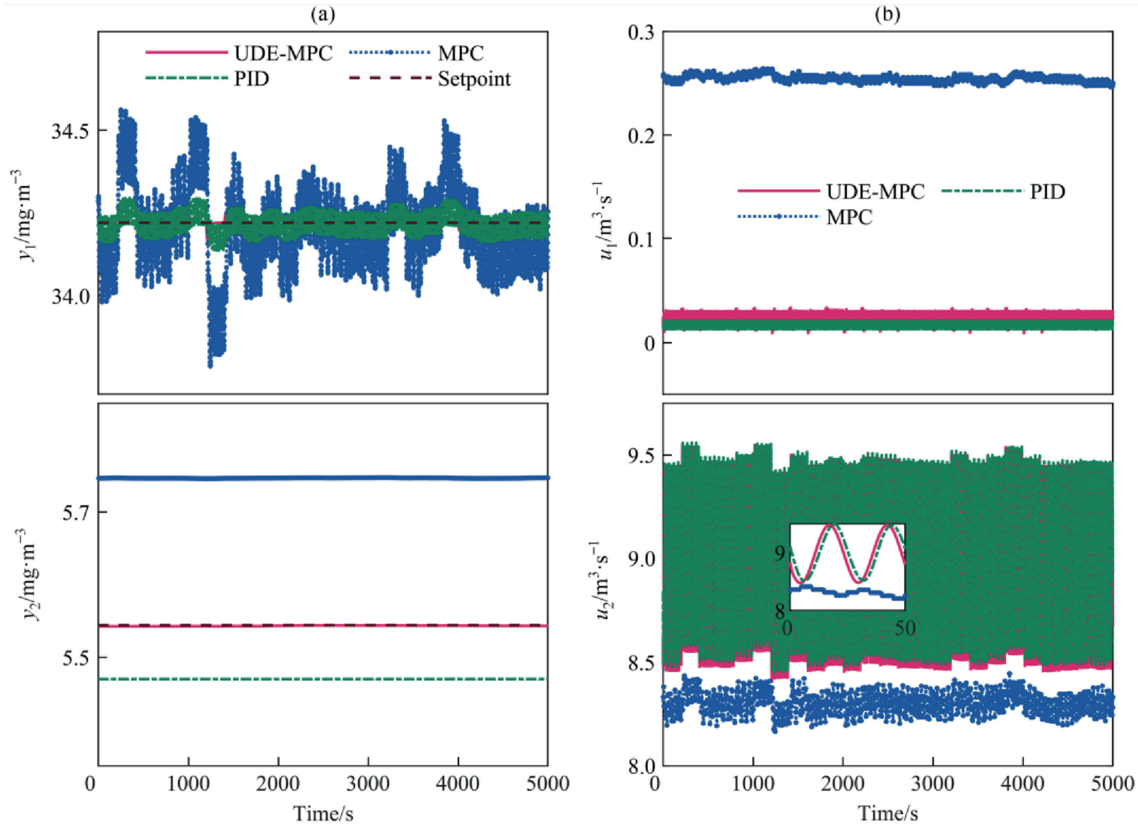

Fig. 7. The desulphurization system simulation results in the presence of large-amplitude external disturbances under different control schemes, with: (a) response curves of controlled variables and (b) variations of manipulated variables.

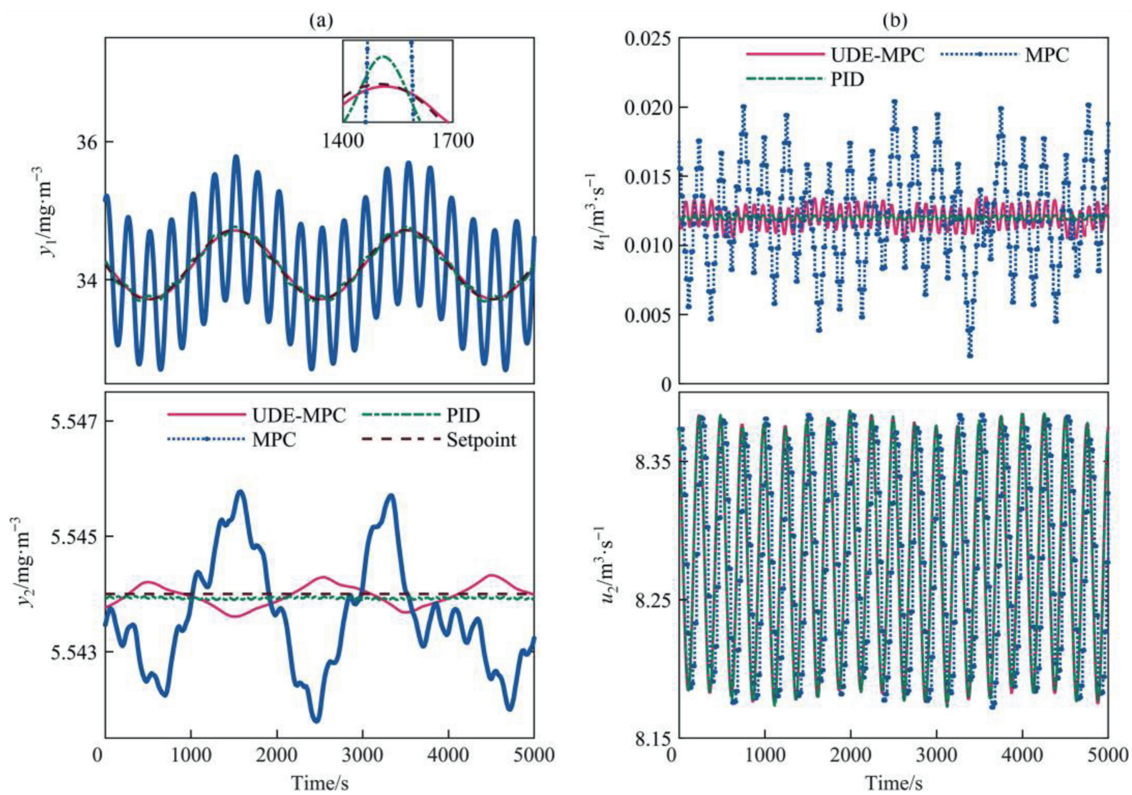

Fig. 8. The desulphurization system simulation results in the presence of small-amplitude external disturbances under different control schemes with varying emission concentration, with (a) response curves of controlled variables and (b) variations of manipulated variables.

4.1.2. Case II: SO_2 emission concentration limit fluctuates

Depending on the emission regulation and economic factors, the SO_2 emission concentration set-point may need to be changed. To compare the robustness of the three considered control techniques against external disturbances while the set-point fluctuates, simulations are performed in cases of small- and large-amplitude disturbances. The parameters of acting disturbances are set the same as in Case I. Both disturbance rejection and emission concentration tracking performance are evaluated. Figs. 8 and 9 show the simulation results of the desulphurization system with different amplitudes of the disturbance, in which the target SO_2 emission concentration varies in the following fashion:

$$y_{1\mathrm{set}} = 34.2 + \sin(2\pi * 0.0005t) \tag{33}$$

Fig. 8(a) shows the SO_2 emission concentration tracking performance with PID, MPC, and proposed UDE-MPC control schemes against system-inherent uncertainties and external disturbances and under varying set-points. The tracking performance of the proposed control scheme seems almost insensitive to the external disturbances. The SO_2 emission concentration is regulated near the set-point and fluctuates within 0.0376 $mg \cdot m^{-3}$, regardless of the external disturbance and the set-point fluctuation. It illustrates that the UDE is working correctly in fast and accurate estimation and compensation of the nonlinearity and parameter coupling. The SO_2 emission concentration in case of standard MPC always remains far from the set-point, which is due to the input action delay caused by the feedback compensation.

Figs. 8 and 9 and Table 2 show that the disturbance amplitude has an effect on the performance of the controller, but the disturbance rejection performance of the proposed UDE-MPC control scheme is significantly better than that of the other two controllers, thus showing less model dependence. The larger the disturbance amplitude, the more obvious this advantage is. The tracking performance of the standard MPC controller varies considerably with the amplitude of the disturbance, whereas the variations in case of UDE-MPC controller can almost be ignored. In other words, the proposed control scheme can considerably minimize output fluctuation and improve dynamic performance in both scenarios of sinusoidal and constant-target SO_2 emission concentration. Besides, the pH value of the slurry under the three tested control methods can meet the requirements of safe production.

Table 2
Tracking error of SO_2 between different control schemes

Performance index	Small-amplitude disturbance			Large-amplitude disturbance		
	PID	MPC	UDE-MPC	PID	MPC	UDE−MPC
ATE/$mg \cdot m^{-3}$	0.0316	0.6431	0.0249	0.1592	4.2422	0.0478
MTE/$mg \cdot m^{-3}$	0.0536	1.1026	0.0376	0.2895	9.0911	0.2177

4.2. Effects of time constant on disturbance suppression

Most of the disturbances in the desulphurization system concentrate at low frequencies, but the system response differs with the frequency. In this section, several controllers are designed with different filter time constants to suppress the external disturbances and desirably obtain a control scheme that can fully meet the system-desired disturbance rejection performance. First, the external disturbance with different frequencies is used, and the

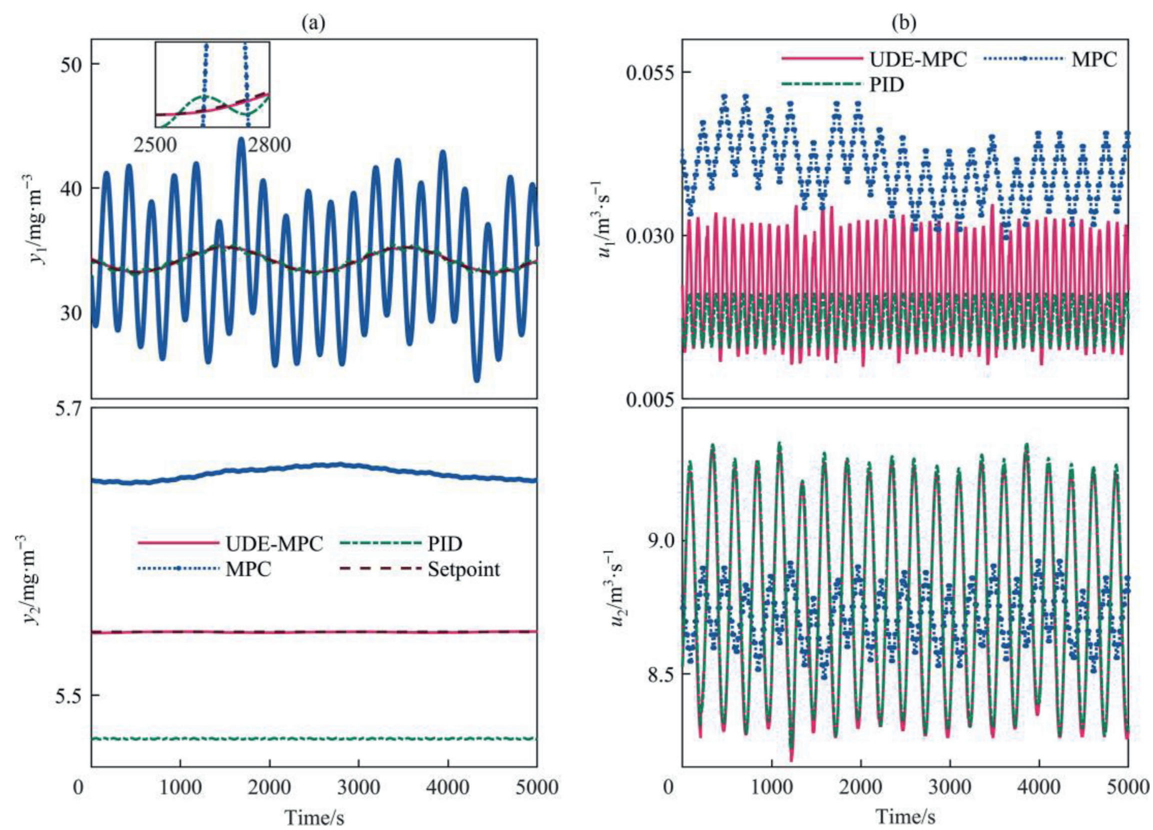

Fig. 9. The desulphurization system simulation results in the presence of large-amplitude external disturbances under different control schemes with emission concentration varies, with (a) response curves of controlled variables and (b) variations of manipulated variables.

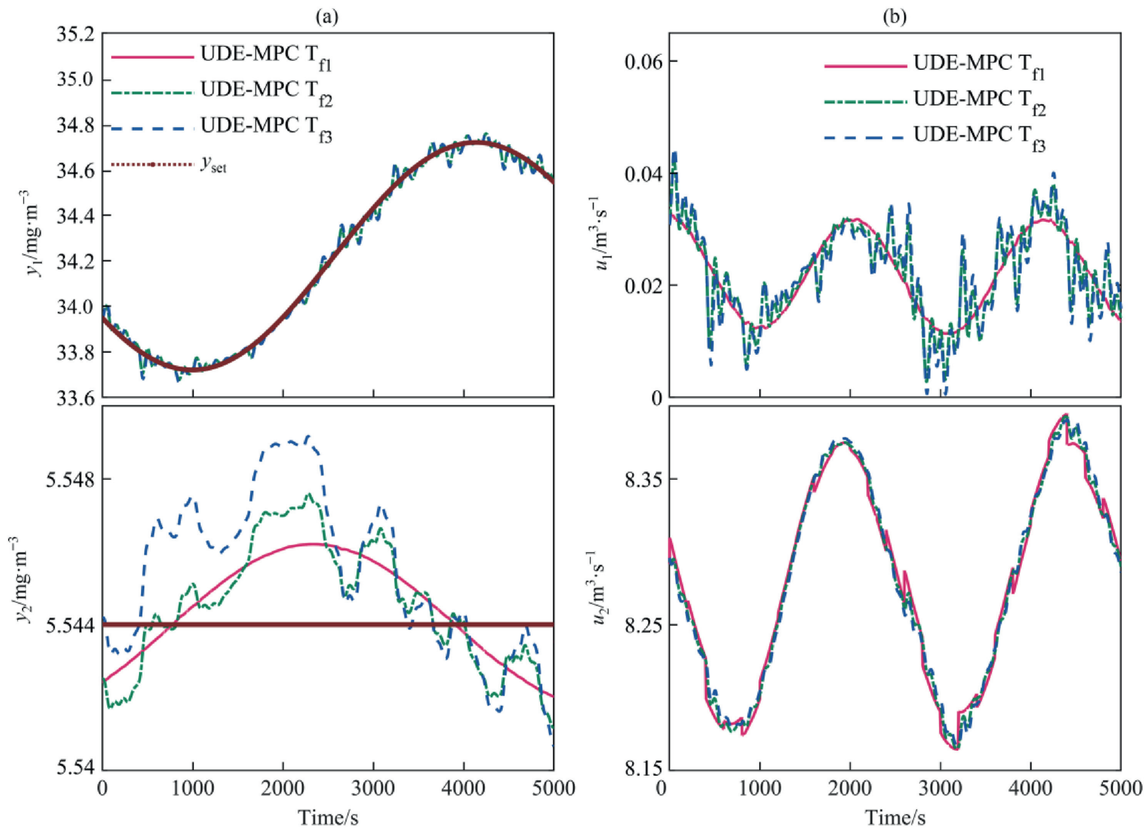

Fig. 10. Robustness under sinusoidal tracking with different filter time constant, with (a) response curves of controlled variables and (b) variations of manipulated variables.

disturbance rejection performance is observed by adjusting the bandwidth of the filter. It should be noticed that the external disturbance will effectively limit the ability of the controllers to reach the performance that the desulphurization system requires. Fig. 10 shows that the filter time constant has a significant impact on the desulphurization system dynamics. The decrease of the filter time constant leads to less tracking error and better robustness. Theoretically, a small filter time constant allows for the estimation and compensation of a wide frequency range of disturbances and uncertainty. In practice, however, it is difficult to set the T_f vlue very small; therefore, a compromise should be chosen to make the filter cover the most disturbance.

5. Conclusions

In this paper, the problem of governing a nonlinear, disturbed, and uncertain desulphurization process was studied under the MPC scheme. To overcome the strong nonlinear behavior of the process as well as to improve the disturbance rejection of the desulphurization process control system, an UDE has been incorporated into the MPC structure. Under the proposed UDE-MPC scheme, the model nonlinearity, external disturbances, and system coupling could be regarded as a lumped uncertainty term, chiefly simplifying the controller synthesis. The obtained simulation results verified the capability of disturbance estimation and compensation of the proposed control scheme in different disturbance-related scenarios. Compared to the standard MPC and PID algorithms, the introduced UDE-MPC approach has shown improved tracking performance and robustness. Furthermore, it was found that the tracking error could be further decreased by decreasing (to some extent) the filtering time constant.

The operation process of the desulphurization system is complex, and this paper addresses common disturbance and model-mismatch problems while acknowledging its limitation of not accounting for unbounded disturbances and input delays. To enhance the control performance of current robust controllers for desulphurization systems, these are all crucial issues that attract our attention and will be the focus of our future research.

Declaration of Interest

The authors declare that they have no known competing financial interests or personal relationships that could have appeared to influence the work reported in this paper.

Acknowledgements

This work was supported by the key project of the National Nature Science Foundation of China (51736002).

Nomenclature

A	specific surface area, $m^2 \cdot g^{-1}$
C	liquid phase molar concentration, $mol \cdot m^{-3}$
G	flue gas flow rate, $m^3 \cdot s^{-1}$
G_{air}	oxidation air flow rate, $m^3 \cdot s^{-1}$
H	Henry constant
K_G	total mass transfer coefficient, $mol \cdot m^{-2} \cdot s^{-1} \cdot Pa^{-1}$
K_{SP}	solubility rate constant, $(mol \cdot m^{-3})^2$
$k_{d,CaCO_3}$	dissolution rate constant, $mol \cdot m^{-3} \cdot s^{-1}$
k_G	gas phase mass transfer coefficient, $mol \cdot m^{-2} \cdot s^{-1} \cdot Pa^{-1}$

k_L	liquid phase mass transfer coefficient, $m \cdot s^{-1}$
k_{ox}	oxidation rate constant, $(m^3 \cdot mol^{-1})^{1.5} \cdot s^{-1}$
L	dissolution equilibrium constant, $(mol \cdot m^{-3})^2$
M	molar mass, $kg \cdot mol^{-1}$
$m_{SO_2,in}$	SO_2 concentration of inlet flue gas, $mol \cdot m^{-3}$
$m_{SO_2,out}$	SO_2 concentration of clean gas entering chimney, $mol \cdot m^{-3}$
P	inlet pressure of flue gas, Pa
p	partial pressure in gas phase pressure, Pa
Q	liquid phase flow rate, $m^3 \cdot s^{-1}$
r_c	crystalline rate, $mol \cdot m^{-3} \cdot s^{-1}$
r_d	solution rate, $mol \cdot m^{-3} \cdot s^{-1}$
r_{ox}	oxidation rate, $mol \cdot m^{-3} \cdot s^{-1}$
r_{SO_2}	SO_2 absorption rate, $mol \cdot m^{-3} \cdot s^{-1}$
V_{ta}	slurry volume in oxidation tank, m^3
W_{SO_2}	SO_2 absorbed from the flue gas, $kg \cdot h^{-1}$
W_{CaCO_3}	calcium carbonate consumed, $kg \cdot h^{-1}$
y_{pH}	pH value of the slurry
α	Gas-liquid specific area in spray tower, $m^2 \cdot m^{-3}$
α_T	Gas-liquid specific area in oxidation tank, $m^2 \cdot m^{-3}$
β	enhancement factor
η	the desulphurization efficiency
ρ	density, $kg \cdot m^{-3}$
τ	movement time of droplets, s

Subscripts

fal	falling slurry in absorption zone
i	component i
in	the slurry that entering the oxidation tank
out	the slurry that exhausted from oxidation tank
r	recycled slurry

References

[1] I. Ahmed, S.H. Jhung, Adsorptive desulfurization and denitrogenation using metal-organic frameworks, *J. Hazard. Mater.* 301 (2016) 259–276.

[2] J. Liu, M.S. Tomassone, X.Y. Kuang, S.H. Zhou, Operation parameters and design optimization based on CFD simulations on a novel spray dispersion desulfurization tower, *Fuel Process. Technol.* 209 (2020) 106514.

[3] R. Chen, T.S. Zhang, Y.Q. Guo, J.W. Wang, J.X. Wei, Q.J. Yu, Recent advances in simultaneous removal of SO_2 and NO_x from exhaust gases: Removal process, mechanism and kinetics, *Chem. Eng. J.* 420 (2021) 127588.

[4] B. Guo, A.L. Ren, J. Gao N, Z. Fang, T.Y. Zhu, Sintered flue gas semidry processing desulphurization ash as cementing materials, in: 2009 3rd International Conference on Bioinformatics and Biomedical Engineering, IEEE, Beijing, China, 2009.

[5] T.S. Zhang, C. Wu, B. Li, J.W. Wang, R. Ravat, X.Z. Chen, J.X. Wei, Q.J. Yu, Linking the SO_2 emission of cement plants to the sulfur characteristics of their limestones: A study of 80 NSP cement lines in China, *J. Clean. Prod.* 220 (2019) 200–211.

[6] I.I. Oecd, Energy and Air Pollution: World Energy Outlook Special Report 2016, 2016.

[7] X.L. Han, X.X. Chen, Resource-based method for realizing zero emission of sulfur dioxide from flue gas, in: Proceedings of the 3rd 2017 International Conference on Sustainable Development (ICSD 2017), Atlantis Press, Paris, France, 2017.

[8] Z.G. Shen, X. Chen, M. Tong, S.P. Guo, M.J. Ni, J. Lu, Studies on magnesium-based wet flue gas desulfurization process with oxidation inhibition of the byproduct, *Fuel* 105 (2013) 578–584.

[9] Z.X. Zhu, Y.P. Ma, Z. Qu, L. Fang, W.Y. Zhang, N.Q. Yan, Study on a new wet flue gas desulfurization method based on the Bunsen reaction of sulfur-iodine thermochemical cycle, *Fuel* 195 (2017) 33–37.

[10] L. Koech, H. Rutto, L. Lerotholi, R.C. Everson, H. Neomagus, D. Branken, A. Moganelwa, Spray drying absorption for desulphurization: A review of recent developments, *Clean Technol. Environ. Policy* 23 (6) (2021) 1665–1686.

[11] A.L. Villanueva Perales, F.J. Gutiérrez Ortiz, P. Ollero, F. Muñoz Gil, Controllability analysis and decentralized control of a wet limestone flue gas desulfurization plant, *Ind. Eng. Chem. Res.* 47 (24) (2008) 9931–9940.

[12] Z.K. Yang, C.Y. Liu, X.L. Song, Z.Y. Song, Z.S. Wang, Application of RBF neural network PID in wet flue gas desulfurization of thermal power plant, in: 2016 International Conference on Machine Learning and Cybernetics (ICMLC), 2016, IEEE, Jeju, Korea (South), 2017.

[13] A.L. Villanueva Perales, P. Ollero, F.J. Gutiérrez Ortiz, A. Gómez-Barea, Model predictive control of a wet limestone flue gas desulfurization pilot plant, *Ind. Eng. Chem. Res.* 48 (11) (2009) 5399–5405.

[14] Y.T. Shi, D.H. Sun, Z.J. Li, N.S. Chen, W. Qing, D.J. Gao, Hybrid modeling and control of nonlinear wet flue gas desulphurization process, in: 2007 International Conference on Machine Learning and Cybernetics, IEEE, Hong Kong, China, 2007.

[15] M. Kuure-Kinsey, B.W. Bequette, Multiple model predictive control strategy for disturbance rejection, *Ind. Eng. Chem. Res.* 49 (17) (2010) 7983–7989.

[16] A.L. Villanueva Perales, F.J. Gutiérrez Ortiz, F. Vidal Barrero, P. Ollero, Using neural networks to address nonlinear pH control in wet limestone flue gas desulfurization plants, *Ind. Eng. Chem. Res.* 49 (5) (2010) 2263–2272.

[17] B.Y. Zhu, B. Li, Z. Wang, R.F. Song, S.L. Qiu, Automatic adjustment and optimization of desulphurization slurry supply for 335 MW unit, in: 2019 IEEE 3rd Advanced Information Management, Communicates, Electronic and Automation Control Conference (IMCEC), 2019, IEEE, Chongqing, China, 2020.

[18] X.L. Li, Q.B. Liu, K. Wang, F.Q. Wang, G.M. Cui, Y. Li, Intelligent partition of operating condition-based multi-model control in flue gas desulfurization, *IEEE Access* 8 (2020) 149301–149315.

[19] S. Kambale, S. George, P.R.G. Zope, Controllers used in pH neutralization process: A review, *IRJET* 2 (3) (2015) 354–361.

[20] J.Q. Han, From PID to active disturbance rejection control, *IEEE Trans. Ind. Electron.* 56 (3) (2009) 900–906.

[21] C. Johnson, Further study of the linear regulator with disturbances: The case of vector disturbances satisfying a linear differential equation, *IEEE Trans. Autom. Contr.* 15 (2) (1970) 222–228.

[22] P.O. Larsson, F. Casella, F. Magnusson, J. Andersson, M. Diehl, J. Åkesson, A framework for nonlinear model-predictive control using object-oriented modeling with a case study in power plant start-up, in: 2013 IEEE Conference on Computer Aided Control System Design (CACSD), 2013, Hyderabad, India, IEEE, 2013.

[23] C. Shang, F.Q. You, A data-driven robust optimization approach to scenario-based stochastic model predictive control, *J. Process. Contr.* 75 (2019) 24–39.

[24] X.S. Chen, J. Yang, S.H. Li, Q. Li, Disturbance observer based multi-variable control of ball mill grinding circuits, *J. Process. Contr.* 19 (7) (2009) 1205–1213.

[25] J.H. She, X. Xin, Y.D. Pan, Equivalent-input-disturbance approach—Analysis and application to disturbance rejection in dual-stage feed drive control system, *IEEE ASME Trans. Mechatron.* 16 (2) (2011) 330–340.

[26] S.E. Talole, J.P. Kolhe, S.B. Phadke, Extended-state-observer-based control of flexible-joint system with experimental validation, *IEEE Trans. Ind. Electron.* 57 (4) (2010) 1411–1419.

[27] H.W. Zhou, J.H. Xu, C. Chen, X.G. Tian, G.H. Liu, Disturbance-observer-based direct torque control of five-phase permanent magnet motor under open-circuit and short-circuit faults, *IEEE Trans. Ind. Electron.* 68 (12) (2021) 11907–11917.

[28] K.R. Sun, X.L. Wang, R.W. Guo, Stabilization of nonlinear systems with external disturbances using the DE-based control method, *Symmetry* 15 (5) (2023) 987.

[29] Q.C. Zhong, D. Rees, Control of uncertain LTI systems based on an uncertainty and disturbance estimator, *J. Dyn. Syst. Meas. Contr.* 126 (4) (2004) 905–910.

[30] L. Sun, D.H. Li, Q.C. Zhong, K.Y. Lee, Control of a class of industrial processes with time delay based on a modified uncertainty and disturbance estimator, *IEEE Trans. Ind. Electron.* 63 (11) (2016) 7018–7028.

[31] J.P. Kolhe, M. Shaheed, T.S. Chandar, S.E. Talole, Robust control of robot manipulators based on uncertainty and disturbance estimation, *Int. J. Robust Nonlinear Contr.* 23 (1) (2013) 104–122.

[32] S. Oucheriah, Robust control of the DC–DC boost converter based on the uncertainty and disturbance estimator, *Int. J. Electron.* 104 (11) (2017) 1810–1822.

[33] R. Sanz, P. Garcia, Q.C. Zhong, P. Albertos, Robust control of quadrotors based on an uncertainty and disturbance estimator, *J. Dyn. Syst. Meas. Contr.* 138 (7) (2016) 071006.

[34] L.F. Xiao, Aeroengine multivariable nonlinear tracking control based on uncertainty and disturbance estimator, *J. Eng. Gas Turbines Power* 136 (12) (2014) 121601.

[35] P. Selvaraj, O.M. Kwon, S.H. Lee, R. Sakthivel, Uncertainty and disturbance rejections of complex dynamical networks *via* truncated predictive control, *J. Frankl. Inst.* 357 (8) (2020) 4901–4921.

[36] Y. Zhong, X. Gao, W. Huo, Z.Y. Luo, M.J. Ni, K.F. Cen, A model for performance optimization of wet flue gas desulfurization systems of power plants, *Fuel Process. Technol.* 89 (11) (2008) 1025–1032.

[37] P. Córdoba, Status of Flue Gas Desulphurisation (FGD) systems from coal-fired power plants: Overview of the physic-chemical control processes of wet limestone FGDs, *Fuel* 144 (2015) 274–286.

[38] L.E. Kallinikos, E.I. Farsari, D.N. Spartinos, N.G. Papayannakos, Simulation of the operation of an industrial wet flue gas desulfurization system, *Fuel Process. Technol.* 91 (12) (2010) 1794–1802.

[39] C. Brogren, H.T. Karlsson, Modeling the absorption of SO_2 in a spray scrubber using the penetration theory, *Chem. Eng. Sci.* 52 (18) (1997) 3085–3099.

[40] S. Kiil, M.L. Michelsen, K. Dam-Johansen, Experimental investigation and modeling of a wet flue gas desulfurization pilot plant, *Ind. Eng. Chem. Res.* 37 (7) (1998) 2792–2806.

[41] M.S. Chiu, Y. Arkun, A new result on Relative Gain Array, Niederlinski Index and decentralized stability condition: 2×2 plant cases, *Automatica* 27 (2) (1991) 419–421.

[42] N.L. Ricker, Adaptive optimal control: the thinking man's GPC, *Automatica* 29 (3) (1993) 798–800.
[43] S.S. Keerthi, E.G. Gilbert, Optimal infinite-horizon feedback laws for a general class of constrained discrete-time systems: Stability and moving-horizon approximations, *J. Optim. Theory Appl.* 57 (2) (1988) 265–293.
[44] H. Michalska, D.Q. Mayne, Robust receding horizon control of constrained nonlinear systems, *IEEE Trans. Autom. Contr.* 38 (11) (1993) 1623–1633.
[45] D.Q. Mayne, J.B. Rawlings, C.V. Rao, P.O.M. Scokaert, Constrained model predictive control: Stability and optimality, *Automatica* 36 (6) (2000) 789–814.
[46] Z. Jabbour, S. Moreau, A. Riwan, G. Champenois, Speed estimation comparison between full order state observer & Kalman filter for a haptic interface, in: 2009 IEEE International Symposium on Industrial Electronics, IEEE, Seoul, Korea (South), 2009.
[47] H. Ji, S. Wang, S.R. Huang, Research of permanent magnet servo system based on disturbance observer and Kalman filter, in: 2016 35th Chinese Control Conference (CCC), IEEE, Chengdu, China, 2016.
[48] L. Sun, D.H. Li, K.Y. Lee, Enhanced decentralized PI control for fluidized bed combustor *via* advanced disturbance observer, *Contr. Eng. Pract.* 42 (2015) 128–139.